Carbohydrate Polymers 98 (2013) 257–269

Contents lists available at SciVerse ScienceDirect

Carbohydrate Polymers

journal homepage: www.elsevier.com/locate/carbpol

Synthesis of interpenetrating network hydrogel from poly(acrylic acid-co-hydroxyethyl methacrylate) and sodium alginate: Modeling and kinetics study for removal of synthetic dyes from water

Bidyadhar Mandal[a], Samit Kumar Ray[b,*]

[a] Department of Chemistry, Bijoy Krishna Girls' College, Howrah, India
[b] Department of Polymer Science and Technology, University of Calcutta, 92, A.P.C. Road, Kolkata 700009, India

ARTICLE INFO

Article history:
Received 17 March 2013
Received in revised form 30 May 2013
Accepted 31 May 2013
Available online 10 June 2013

Keywords:
IPN
Sodium alginate
Swelling and network parameters
Dye adsorption
Thermodynamics
Regeneration

ABSTRACT

Several interpenetrating network (IPN) hydrogels were made by free radical *in situ* crosslink copolymerization of acrylic acid (AA) and hydroxy ethyl methacrylate in aqueous solution of sodium alginate. N,N′-methylenebisacrylamide (MBA) was used as comonomer crosslinker for making these crosslink hydrogels. All of these hydrogels were characterized by carboxylic content, FTIR, SEM, XRD, DTA–TGA and mechanical properties. Swelling, diffusion and network parameters of the hydrogels were studied. These hydrogels were used for adsorption of two important synthetic dyes, i.e. Congo red and methyl violet from water. Isotherms, kinetics and thermodynamics of dye adsorption by these hydrogels were also studied.

1. Introduction

Hydrogels are crosslinked hydrophilic polymer capable of showing extensive swelling in water. Hydrogels are used as effective adsorbent for various applications including agriculture, horticulture, personal care products, drug delivery, separation of heavy metal ions and dye molecules from water, etc. (Wang, Zhang, & Wang, 2011). These superadsorbent polymers are prepared by crosslinking synthetic or natural polymers. Natural polymers are available in large quantities in nature and these biopolymers are also biodegradable and non toxic. Thus, much attention is being presently paid for making biopolymer based hydrogels. Cellulose, the most abundant renewable resource on earth, is the origin for most of the biopolymers (Chang, Duan, Cai, & Zhang, 2010; Peppas, Hilt, Ali, & Robert, 2006). Cellulose having abundant hydroxyl groups can be used to prepare hydrogels easily with fascinating structures and properties. Sodium alginate is a water soluble salt of alginic acid, a natural polysaccharide of brown algae. This non-toxic natural polysaccharide contains 1,4-linked-D-mannuronic acid and L-guluronic acid residues that are arranged in the polymer chain in blocks. These homogeneous blocks are separated by blocks made of random or alternating units of mannuronic and guluronic acids (Peppas et al., 2006). The gelation and cross-linking of alginate is achieved by the exchange of sodium ions with multivalent cations. Such a cross-linked hydrogel is useful in controlled release of bioactive molecules. However, like most of the biopolymer based hydrogels, sodium alginate based hydrogels are also of poor mechanical strength (Jeon, Lei, & Kim, 2008). Properties of sodium alginate based hydrogel may be improved by physical or chemical modification. Jeon et al. incorporated polyaspartate in the matrix of sodium alginate and used this composite hydrogel for adsorption of malachite green and methyl orange from water (Jeon et al., 2008). Yin et al. grafted sodium alginate with acrylic acid and hydrogel was prepared by crosslinking this graft copolymer with MBA. This hydrogel showed excellent swelling characteristics in different buffer solutions (Yin, Ji, Dong, Ying, & Zheng, 2008). Hua et al. prepared hydrogel by freeze thawing blend of polyvinyl alcohol and sodium alginate. This hydrogel was investigated for controlled release of diclofenac sodium (Huaa, Mac, Xun, Yanga, & Wanga, 2010). IPN type hydrogel based on a natural polymer and a petrochemical based synthetic polymer could result in materials, which combine the mechanical properties of the synthetic polymer with the biological properties of the natural polymer. IPN polymers consist of two or more polymers where at least one polymer is crosslinked. Due to entanglement of the networks of the constituent polymers, IPN based hydrogels are of excellent mechanical strength. In recent times various IPN type hydrogels based on sodium alginate

* Corresponding author. Tel.: +91 33 23508386; fax: +91 33 23519755.
E-mail address: samitcu2@yahoo.co.in (S.K. Ray).

0144-8617/$ – see front matter © 2013 Elsevier Ltd. All rights reserved.
http://dx.doi.org/10.1016/j.carbpol.2013.05.093

were synthesized for different applications. Solpan et al. prepared semi-IPN of sodium alginate and acrylamide and used this hydrogel for separation of several textile dyes from water (Dilek, Murat, & Guven, 2008). Kulkarni et al. synthesized IPN of polyvinyl alcohol and sodium alginate and used it for controlled release of prazosin hydrochloride from skin (Kulkarni, Sreedhara, Mutalikb, Setty, & Sa, 2010). Wang and Wang grafted sodium alginate with sodium acrylate and prepared semi-IPN with this grafted copolymer and polyvinyl pyrolidone. This semi-IPN hydrogel was pH sensitive and showed good swelling properties (Wang & Wang, 2010). Horia et al. prepared IPN of sodium alginate and polyacrylic acid by gama radiation. These hydrogels showed excellent sorption for heavy metal ions such as copper, cobalt and nickel (Horia et al., 2008).

It transpires from the above discussion that IPN of sodium alginate has been used as adsorbent for various applications. In the present work acrylic acid and hydroxy ethyl methacrylate monomers were copolymerized *in situ* in the matrix of water soluble sodium alginate by free radical polymerization. The copolymer was crosslinked with MBA. Accordingly, several semi-IPNs were made by varying crosslinker concentration, initiator concentration and % of sodium alginate in water. For these hydrogels molar ratio of acrylic acid and hydroxy ethyl methacrylate was fixed at 5:1. IPN were also made by copolymerizing sodium acrylate and hydroxy ethyl methacrylate in sodium alginate with same comonomer ratio (5:1). These semi-IPN hydrogels were characterized by carboxylic content, swelling characteristics, network parameters, FTIR, SEM, XRD, DTA–TGA and mechanical properties. These hydrogels were used for adsorption of two important synthetic dyes, i.e. Congo red and methyl violet from water. Both of these industrial dyes are extensively used for coloring products (Banat, Nigam, Singh, & Marchant, 1996; Li, Xu, Wang, Chen, & Feng, 2009). These dyes are highly soluble in water with high tinctorial values. Further, because of the presence of complex aromatic rings in its structures, these dyes are not biodegradable (Li et al., 2009). Thus, in the present work the semi-IPN hydrogels were used for adsorption of these industrially important synthetic dyes from water.

2. Materials and methods

2.1. Materials

Monomers i.e. acrylic acid (from Fluka), hydroxyethyl methacrylate (from Fluka), N,N′-methylenebisacrylamide (MBA, from Fluka), redox initiator pair i.e. ammonium persulfate (APS, from Fluka), sodium metabisulfite (SMBS, Merck), Congo red and methyl violet dye were of analytical grade and used without further purification. Natural polymer sodium alginate (average molecular weight 500,000 and degree of deacetylation 84%) was procured from Merck and used as it is without any further purification.

2.2. Methods

2.2.1. Preparation of hydrogel

Copolymer hydrogels were prepared by free radical cross-link copolymerization of acrylic acid and hydroxyl ethyl methacrylate in presence of crosslinker comonomer MBA. The polymerization reaction was carried out in a three necked glass reactor equipped with a mechanical stirrer, reflux condenser and thermometer. The dissolved oxygen of the reaction mixtures was removed by purging nitrogen gas for half an hour in the reaction mixtures before addition of the reacting monomers and crosslinker. After addition of the monomers and crosslinker the temperature of the reaction mixtures was raised to 60 °C with addition of required amounts of redox pair of initiator i.e. ammonium persulfate and sodium metabisulfite. The reaction was then continued at this temperature till the reaction mixtures gelled. For synthesizing the IPN hydrogel, the hydrophilic natural polymer i.e. sodium alginate was first dissolved in water well for half an hour followed by addition of monomers to this viscous solution and stirring for another half an hour. Copolymerization of acrylic acid and hydroxy ethylmethacrylate were allowed in the solution of sodium alginate in a similar way as in the case of copolymerization of acrylic acid and hydroxy ethylmethacrylate in water. The gel obtained was disintegrated in a blender, washed with water and then isopropyl alcohol, followed by filtration and finally dried to constant weight at 30 °C in a vacuum oven. For synthesizing the IPN hydrogel of sodium salt, sodium acrylate was first made by drop wise addition of 1 M acrylic acid to 1 M sodium hydroxide solution in water kept on an ice bath till complete neutralization occurs. Four kinds of hydrogels as obtained by the above reaction i.e. the hydrogel obtained from copolymer of acrylic acid and hydroxy ethylmethacrylate, sodium acrylate and hydroxy ethyl methacrylate, IPN of copolymer of acrylic acid and hydroxy ethylmethacrylate with sodium alginate and IPN of copolymer of sodium acrylate and hydroxy ethyl methacrylate with sodium alginate were designated as CP, SCP, $CPSA_x$ and $SCPSA_x$, respectively where x is % of sodium alginate in the IPN.

2.2.1.1. Gel content of the hydrogel. The hydrogels as synthesized above were dried in a vacuum oven at ambient temperature to a constant weight (W_i). The dried sample was then kept in deionized water for a week with occasional shaking to remove the water soluble uncrosslink and low molecular weight substances from the gel. It was then taken out from water. This water insoluble gel sample was further dried in vacuum oven to a constant weight (W_d). The percent gelation of IPN gels were obtained as

$$\text{Gel\%} = \frac{W_d}{W_i} \times 100 \quad (1)$$

2.2.2. Characterization of the hydrogels

The synthesized hydrogels were characterized by the following methods.

2.2.2.1. Determination of carboxylic groups present in the hydrogels. Total amount of free carboxylic groups (COOH, mass% of hydrogel) present in the hydrogels were determined by a method reported elsewhere (Mall, Srivastava, Kumar, & Mishra, 2006; Mandal, Ray, & Bhattacharyya, 2012). Around 0.5 g of hydrogel sample (w) was taken in 25 mL 0.1 M NaOH solution and after mixing under magnetic stirring for 2 h it was titrated with 0.1 M HCl solutions. The amount of carboxylic groups (mass%) in the hydrogel was calculated as

$$C = [(C_{\text{NaOH}} \times V_{\text{NaOH}} - C_{\text{HCl}} \times V_{\text{HCl}}) \times 45 \times 10^{-3} \times 100] \quad (2)$$

2.2.2.2. Fourier transform infrared spectroscopy (FTIR). FTIR spectra of the copolymer hydrogels were recorded on a FTIR spectrometer (Perkin Elmer, model-Spectrum-2, Singapore) using KBr pellet made by mixing KBr with fine powder of the polymer gel samples (10:1 mass ratio of KBr to polymer).

2.2.2.3. Scanning electron microscopy (SEM). The copolymer and IPN gel samples were coated with gold (Au). The morphology of the gels were observed by using SEM (scanning electron microscope, model no. S3400N, VP SEM, Type-II, made by Hitachi, Japan) with the accelerating voltage set to 15 kV.

2.2.2.4. X-ray diffraction (XRD). The change of crystallinity of sodium alginate by IPN formation was characterized by X-ray diffraction (XRD). Wide angle X-ray diffraction profile of the hydrogel samples were studied at 25 °C with a diffractometer (model:

X'Pert PRO, made by PANalytical B.V., The Netherlands) using Ni-filtered Cu K_α radiation (λ = 1.5418 Å) and a scanning rate of 0.005° (2θ/s). The angle of diffraction was varied from 2° to 72°.

2.2.2.5. DTA–TGA. Differential thermal analysis (DTA) and thermo gravimetric analysis (TGA) of the hydrogel samples were carried out in a Perkin Elmer instrument in nitrogen atmosphere at the scanning rate of 10 °C/min in the temperature range of 60–600 °C.

2.2.2.6. Mechanical properties. The tensile strength (TS) and elongation at break (EAB) of the hydrogel samples were determined by a Lloyd-Tensile tester (Lloyd instruments, England). The experimental procedure for mechanical properties is reported elsewhere (Tang, Sun, Li, Wu, & Lin, 2009). In this work, cubic sample of 2 mm × 2 mm × 80 mm size was used. The crosshead speed of 100 mm/min was maintained. The cubic samples were elongated at a strain rate of 5%/min. The TS and EAB were calculated on the basis of initial cross section area of the sample.

2.2.3. Study of equilibrium swelling and swelling kinetics

For studying dynamic swelling properties of the hydrogels dried hydrogel was weighed (W_d) and immersed in distilled water at room temperature. The swollen hydrogels were withdrawn from the solution at different time intervals (t) and weighed (W_t) after removing excess surface water with filter paper. Each sample was weighed three times to minimize error and the average values of these three measurements were taken. Swelling experiments were continued till the hydrogels reach its equilibrium swelling value (W_e). The swelling ratio (S_t), equilibrium swelling ratio (S_e) and equilibrium water content (EWC) was determined by using the following equations (Murthy, Murali Mohan, Sreeramulu, & Mohana Raju, 2006).

$$S_t \ \ (\mathrm{g/g}) = \frac{W_t - W_d}{W_d} \tag{3a}$$

$$S_e \ \ (\mathrm{g/g}) = \frac{W_e - W_d}{W_d} \tag{3b}$$

$$\mathrm{EWC} \ \ (\mathrm{g/g}) = \frac{W_e - W_d}{W_e} \tag{3c}$$

The swelling experiments were also carried out at different pH (3.5–9) by immersing the hydrogels in buffer solutions. The buffer solutions of varied pH were prepared by dissolving phosphoric acid, potassium phosphate (KH_2PO_4), potassium hydrogen phosphate (K_2HPO_4), sodium chloride and sodium hydroxide in distilled water. Ionic strengths of the buffer solutions were adjusted to 0.1 M with sodium chloride solution. The pH values were determined by a pH meter. Swelling kinetics of the hydrogels was obtained by direct non-linear fitting of swelling data (S_t) of the hydrogels at different time intervals to the following second order rate, Eq. (4) (Mall et al., 2006).

$$S_t = \frac{W_e^2 k_{S2} t}{1 + k_{S2} W_e t} = \frac{r_0 t}{1 + k_{S2} W_e t} \tag{4}$$

Here, k_{s2} is rate constant and r_0 is initial rate of swelling.

2.2.4. Network parameter of the hydrogels

The average molecular weight between crosslinks ($\bar{M}$) of the hydrogel was obtained from swelling data using the following Flory and Rehner equation (Paul & John, 1943).

$$\bar{M} = -\frac{V_s \rho_p (\phi_p^{1/3} - (\phi_p/2))}{\ln(1-\phi_p) + \phi_p + \chi \phi_p^2} \tag{5}$$

The molar volume of water, V_s at experimental temperature (25 °C) was calculated (18.18 cm^3/mole) from its density (0.99 g/cm^3) and molecular weight (18 g/mole), the density of hydrogel sample, ρ_p was calculated from its mass and volume. The volume of the polymer sample was measured by the method reported elsewhere (Mandal, Ray, & Bhattacharyya, 2012). For equilibrium swelling of m_w g water/g dry hydrogel sample, polymer volume fraction in swollen gel under equilibrium, ϕ_p will be

$$\phi_p = \left(1 + \frac{\rho_p}{\rho_i} m_w\right)^{-1} \tag{6}$$

Here, ρ_p and ρ_i are density of polymer and solvent (water), respectively.

The polymer–solvent interaction parameter, χ between water and polymer hydrogel is obtained using the following equation (Xue, Champ, & Huglin, 2001).

$$\chi = \frac{V_p}{3} + 0.5 \tag{7}$$

Crosslink density (ρ_c) of a hydrogel is obtained as (Sunil & Surinderpal, 2006).

$$\rho_c = \frac{\rho_p N_A}{\bar{M}} \tag{8}$$

N_A is Avagadro's number (6.023×10^{23}/mol). The mesh size (ς in Å) of the swollen polymeric network is calculated from the following equation (Canal & Peppas, 1989).

$$\varsigma = \left[C_n \left(\frac{2\bar{M}}{M_r}\right)\right]^{1/2} l \phi_p^{-1/3} \tag{9}$$

The Flory's characteristic ratio, C_n was taken from literature as 2 (Morris, Cutler, Ross-Murphy, Rees, & Price, 1981) and C—C bond length; 'l' was assumed as 1.54 Å (Mandal et al., 2012). M_r, the molecular weight of repeat unit was calculated as the weight average of the repeat unit of sodium alginate (M_r = 198), PAA (M_r = 72) and hydroxy ethylmethacrylate (M_r = 132). The values of all of these network parameters of the semi and full IPN hydrogels were calculated using Eqs. (4)–(9) and these values are given in Table 1.

2.2.5. Diffusion kinetics through the hydrogels

For understanding the nature of diffusion of water through hydrogels, diffusion constant (k_D) and diffusional exponent (n) was obtained from fractional water uptake (F) using the following equation (Ritger & Peppas, 1987).

$$F = \frac{W_t}{W_e} = k_D t^n \tag{10}$$

Diffusion coefficient (D) of water through cylindrical hydrogels of radius r was obtained from k and n using the following equation (Ritger & Peppas, 1987).

$$D = \pi r^2 \left(\frac{k}{4}\right)^{1/n} \tag{11}$$

2.2.6. Study of dye removal capacity of the hydrogels

Solutions of the two kinds of dye, i.e. Congo red (CR) and methyl violet (MV) with varied concentration range (10–140 mg/l) were prepared in distilled water. 50 mg of hydrogel was taken in 50 cm^3 of the dye solution with continuous stirring on a magnetic stirrer until equilibrium was reached. After equilibrium was reached, the dye solution was separated by decantation from the hydrogel. The concentration of dye solutions before and after addition of hydrogel were determined by spectrophotometric measurement from a pre-calibrated curve of absorbance versus concentrations using Perkin Elmer lamda 2 5 UV-visible Spetrophotometer. The absorbance of the dye solutions was measured at wavelength of 497 nm for CR and 586 nm for MV dye. The amount of dye uptake (in mg) by unit mass (in g) of the hydrogel at equilibrium (Q_e, mg/g) and adsorption or removal % (R%) was calculated using the following equations.

$$Q_e = \frac{(C_0 - C_e)V}{m} \tag{12}$$

Table 1
Swelling diffusion and network parameters of the hydrogels.

Polymer	k_{s2} ($\times 10^4/r_0$)	EWC_{expt}/EWC_{cal} (g/g)	$r^2/\chi^2/F$	$k_D/n/D$ ($\times 10^{10}$)	$r^2/\chi^2/F$	$\bar{M}$ ($\times 10^{-5}$)/ρ_c ($\times 10^{-18}$)/ς
MBA0.5	6.13/0.04	7.12/8.19	1/0.0012/11361	0.059/0.39/3.7	0.863/0.008/363	21/0.53/765
MBA1	5.86/0.03	6.32/7.29	0.986/0.010/1423	0.068/0.37/3.11	0.988/0.002/1079	14/0.81/601
MBA1.5	7.17/0.02	5.26/5.98	0.997/0.009/1238	0.07/0.35/3.12	0.987/0.002/1082	7.46/1.52/416
MBA2	9.49/0.024	4.56/5.1	0.999/0.007/1893	0.06/0.38/3.88	0.974/0.002/808	4.58/2.47/312
INI1.5	7.29/0.04	6.62/7.44	0.996/0.003/5432	0.083/0.34/2.56	0.881/0.0098/274	.3.8/2.14/288
INI1	5.85/0.031	6.32/7.29	0.986/0.010/1423	0.068/0.37/3.11	0.988/0.002/1079	3.22/2.52/261
INI0.75	5.94/0.025	5.26/6.02	0.993/0.004/3365	0.065/0.37/3.51	0.927/0.0061/420	2.36/3.7/216
INI0.5	13.7/0.028	4.04/4.56	0.983/0.008/1199	0.095/0.32/2.15	0.975/0.002/1079	1.23/7.48/147
SA0	5.85/0.031	2.84/3.29	0.986/0.002/1800	0.06/0.37/3.58	0.887/0.006/479	0.2/39.1/51.98
SA2	5.44/0.028	5.817.23	0.982/0.001/1406	0.057/0.39/4.15	0.955/0.003/1098	6.23/1.62/378
SA4	5.85/0.03	6.32/7.29	0.986/0.010/1423	0.068/0.37/3.11	0.988/0.002/1079	14/0.8/601
SA6	13.04/0.013	6.16/5.25	0.972/0.002/1623	0.05/0.39/4.46	0.908/0.006/406	14.8/0.79/619
SA8	6.11/0.027	5.58/6.75	0.985/0.003/0603	0.05/0.40/4.57	0.916/0.005/472	11.8/1.01/542
SSA0	0.15/0.012	8.96/12.5	0.981/0.275/674	0.015/0.53/5.85	0.927/0.0129/174	11.1/0.74/540
SSA2	0.065/0.008	9.18/13.7	0.992/0.097/1623	0.009/0.58/6.36	0.983/0.0024/779	27.1/0.36/900
SSA4	50.37/0.008	10.08/11.03	0.993/0.105/1656	0.007/0.61/6.6	0.977/0.003/560	59.4/0.18/1416
SSA6	0.067/0.008	7.95/11	0.996/0.036/3428	0.012/0.55/5.59	0.989/0.002/1254	29.9/0.37/942
SSA8	60.047/0.006	7.47/11.9	0.996/0.032/3158	0.007/0.61/7.1	0.988/0.001/1116	30.1/0.39/941
SA4pH3	60/0.018	1.59/1.74	0.985/115/1307	0.19/0.22/0.25	0.978/0.002/1129	0.14/7.86/41.30
SA4pH5	20/0.017	2.58/2.78	0.994/20/1832	0.12/0.27/0.7	0.951/0.005/254	0.66/1.70/100.6
SA4pH7	5.85/0.03	6.32/7.29	0.986/0.010/1423	0.068/0.37/3.11	0.988/0.002/1079	3.22/2.52/261
SA4pH8	3.8/0.058	10.68/12.3	0.993/1684/2022	0.086/0.33/1.66	0.938/0.011/254	89.5/0.01/1795
SA4pH9.5	3.7/0.06	11.4/12.85	0.992/1766/2067	0.088/0.32/1.50	0.971/0.005/606	92.1/0.01/1832
SSA4pH3	0.006/0.002	7.9/6.41	0.993/0.272/1716	0.0006/0.9/13.9	0.965/0.005/350	25/0.04/850
SSA4pH5	70.34/0.006	7.95/9.3	0.994/0.127/2249	0.006/0.63/7.58	0.974/0.00394/490	25.6/0.04/862
SSA4pH7	0.37/0.0085	10.08/11.03	0.992/0.105/1656	0.007/0.60/6.60	0.977/0.003/560	59.4/0.01/1416
SSA4pH8	0.37/0.012	12.11/12.91	0.997/0.027/4093	0.009/0.58/6.61	0.992/0.001/1541	115/0.009/2084
SSA4pH9.5	0.37/0.015	15.37/23.3	0.998/0.017/5037	0.008/0.59/7.1	0.998/0.002/1921	269/0.004/3449

k_{s2} (g gel/g water min), r_0 (g water/g gel min), k_D (s-1), n (−), D (cm^2/s).

$$R\% = \frac{(C_0 - C_e)}{C_0} \times 100 \tag{12a}$$

Here C_0 and C_e are initial and equilibrium concentration of dye solution (mg/l) while V is volume (l) of the dye solution containing the hydrogel and m is mass (g) of the dry hydrogel polymer used for the experiment.

2.2.6.1. Adsorption isotherm. The dye adsorption data (Q_e vs. C_e) was directly fitted to the following non linear two-parameter Langmuir (Langmuir, 1918) isotherm (Eq. (13)) and four-parameter Fritz–Schlünder (Fritz & Schlunder, 1974) isotherms (Eq. (14))

Langmuir isotherm.

$$Q_e = \frac{Q_{max} K_L C_e}{1 + K_L C_e} \tag{13}$$

The characteristic of Langmuir isotherm is expressed in terms of dimensionless separation factor R_L defined as

$$R_L = \frac{1}{K_L + C_o} \tag{13a}$$

where C_o is the maximal dye concentration. For favorable Langmuir adsorption $0 < R_L < 1$.

Fritz–Schlünder (FS) isotherm

Most of the adsorption isotherms are combined in the following generalized four-parameter Fritz–Schlünder isotherm

$$Q_e = \frac{A_{FS} C_e^{\alpha}}{1 + B_{FS} C_e^{\beta}} \tag{14}$$

where A_{FS} and B_{FS} are Fritz–Schlünder constants while α, and β are equation exponent. This model equation is reduced to Sip model when $\alpha = \beta$ and $c = 1$, Redlich–Peterson model when $\alpha = c = 1$, Langmuir model when $\alpha = c = \beta = 1$ and Freundlich model when $c = 0$.

2.2.6.2. Adsorption kinetics. Kinetics of dye adsorption was evaluated by substituting dye adsorption (Q_t) data at different time intervals (t) to the following pseudo second order (Eq. (15)) of Ho and McKay (1999) and intra particle diffusion model (Eq. (16)) of Weber and Morris (1963)

$$Q_t = \frac{Q_e^2 k_2 t}{1 + k_2 Q_e t} \tag{15}$$

$$Q_t = k_p t^{1/2} + c \tag{16}$$

Here k_2 and k_p are rate constant for 2nd order and intra particle diffusion, respectively and c is intercept. The diffusion of dye molecules is only by intra particle diffusion if the trend lines pass through origin (i.e. $c = 0$). For some values of c (i.e. $c \neq 0$) diffusion is controlled by some other mechanisms apart from intra particle diffusion. In fact, the curves following intra particle diffusion have three different stages i.e. initial very fast surface adsorption (external mass transfer) followed by a linear intra particle diffusion and finally a plateau showing equilibrium sorption where intra particle diffusion is very slow due to low concentration of dye (solute) in solution (Kayranli, 2011).

3. Results and discussion

3.1. Synthesis of IPN hydrogels

In the present hydrogels acrylic acid and hydroxy ethylmethacrylate was copolymerized in presence of sodium alginate in water by free radical polymerization. Hydrogel was also made by crosslink copolymerization of acrylic acid and hydroxy ethylmethacrylate with MBA. However, this copolymer hydrogel shows poor mechanical strength due to extensive swelling in water. Thus, in the present work sodium alginate was introduced in the copolymer hydrogel by interpenetration to increase gel strength of the hydrogels. Sodium alginate was chosen since it is a water soluble natural polymer. Sodium alginate contributes to mechanical strength of the gel because of its crystallinity. It also enhances swelling of the IPN gel due to its hydrophilicity. In this polymerization the copolymer was crosslinked by MBA by crosslink

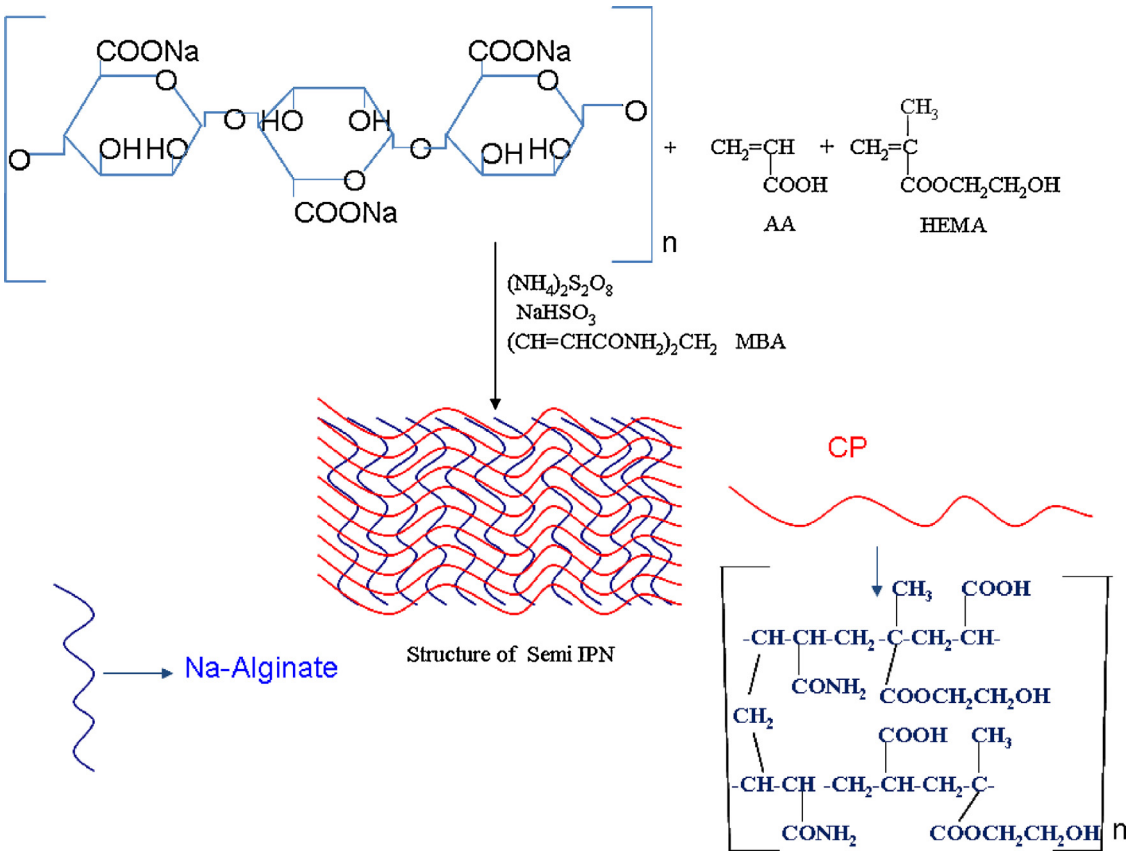

Scheme 1. Formation and structure of semi-IPN hydrogel. SA – sodium alginate, AA – acrylic acid monomer, HEMA – hydroxyethyl methacrylate monomer, MBA – N,N′-methylenebisacrylamide crosslink comonomer, CP – crosslink copolymer, semi-IPN – semi interpenetrating network hydrogel.

copolymerization. These hydrogels are semi interpenetrating since the copolymer is only crosslinked. In this free radical polymerization the bifunctional monomer or crosslinker MBA undergoes copolymerization with both of the other two monomers i.e. acrylic acid and hydroxy ethylmethacrylate to form the crosslink copolymer hydrogel. During polymerization in aqueous medium primary radicals are generated by initiation of redox initiator and monomers i.e. acrylic acid, hydroxy ethylmethacrylate and MBA. Radicals are also generated on sodium alginate and it takes part in propagation reactions of the monomers (Wang & Wang, 2010). Thus, interpenetrating network type polymer hydrogel is formed from growing radicals of monomers and sodium alginate macroradicals. Possible structure of the SIPN type hydrogel is shown in Scheme 1.

3.1.1. *Effect of reaction variables on gel content and gel time*

The variation of gel time and gel% of the hydrogel (CPSA4) containing 4% sodium alginate and copolymer of acrylic acid and hydroxy ethylmethacrylate is shown in Fig. 2A. Initiator concentration was fixed at 1 mass% of total monomers when crosslinker % (mass% of total monomers) was varied. Similarly, crosslinker concentration was fixed at 1 mass% of total monomers when initiator concentration was varied. Effect of sodium alginate on gel time and gel% is shown in Fig. 2B for copolymer of acrylic acid and hydroxy ethyl methacrylate and also for copolymer of sodium acrylate and hydroxy ethylmethacrylate. In this case both crosslinker and initiator concentrations were fixed at 1 mass% of total monomers. It is observed that with increase in crosslinker or initiator concentration gel time and gel% decreases. With increase in crosslinker% gel time decreases since network (gel) in the polymer is formed at a much faster rate in presence of increased amount of MBA crosslinker and gel% decreases because of formation of network at an early stage of polymerization. Increase in initiator concentration also increases rate of polymerization and polymer of shorter chain length (lower molecular weight) is formed. Thus, gelling occurs early during polymerization with shorter gel time and less gel% (Mall et al., 2006). It is observed from Fig. 2B that with increase in % of sodium alginate gel time increases while gel% decreases. As the amount of alginate increases it becomes increasingly difficult for the same amount of crosslinker (MBA) to crosslink copolymer of acrylic acid and hydroxy ethylmethacrylate in the semi-IPN. Thus, gel time increases. Further, in the semi-IPN as there is no crosslinking of alginate, soluble part increases with increasing amount of alginate and hence gel% decreases. It is also observed that gel time increases significantly for copolymer containing sodium acrylate instead of acrylic acid. This may be due to less number of free carboxylic groups present in acrylate IPN.

3.2. *Characterization of the hydrogel*

3.2.1. *Amount of free carboxyl group in the hydrogel*

In the semi-IPN hydrogel, sodium alginate contains sodium salt of carboxylic acid while the copolymer contains carboxylic acid (Scheme 1). Some of the carboxylic groups of acrylic acid form chemical bond (ester linkage) with hydroxyl (OH) groups of hydroxy ethylmethacrylate and alginate in the hydrogels (Mall et al., 2006). The amount of free carboxyl group present in the hydrogel was determined by titrating it with 0.1 M NaOH solutions. It is observed that free carboxylic groups of IPN of only acrylic acid in 4% sodium alginate shows maximum carboxylic % (33.8). Hydrogel of crosslink copolymer of acrylic acid and hydroxy ethylmethacrylate (CP) shows lower carboxylic % (29.8) which is further reduced to 24.3% for IPN of acrylic acid and hydroxy ethylmethacrylate in

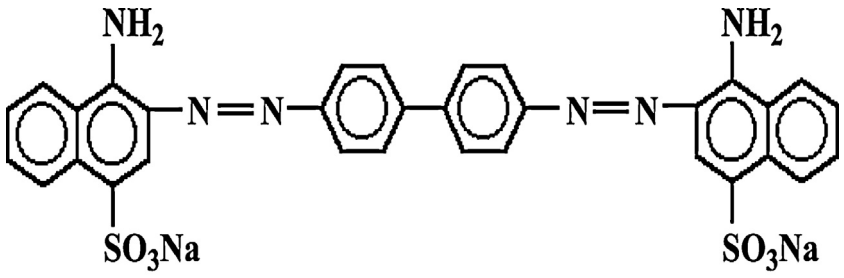

A (Molecular weight- 696.66, Lamda max-497 nm)

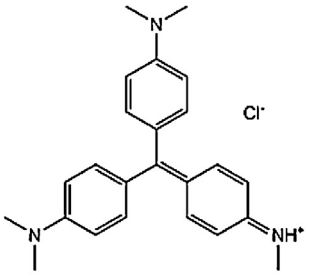

B (Molecular weight- 407.9, Lamda max-586 nm)

Fig. 1. Structure, molecular weight and Lambda max (λ_{max}) of the dye. (A) Congo red and (B) methyl violet.

4% sodium alginate (CPSA4). In this case free carboxylic groups reduce because of presence of hydroxy ethylmethacrylate and thus, reaction of some of the hydroxyl groups of alginate and hydroxy ethylmethacrylate with free carboxylic groups of copolymer. As expected, IPN of sodium salt of copolymer in alginate (SCPSA4) showed minimum carboxylic % (10.9)

3.2.2. FTIR spectroscopy

FTIR spectroscopy was studied to investigate structure of the hydrogels. The FTIR of sodium alginate, copolymer gel of acrylic acid–hydroxy ethylmethacrylate (CP), IPN of this copolymer in 4% sodium alginate (CPSA4), copolymer gel of sodium acrylate and hydroxy ethylmethacrylate (SCP) and IPN of this copolymer in 4% sodium alginate (SCPSA4) is shown in Fig. 3A–E, respectively. As observed in Fig. 3A, sodium alginate shows absorption band at 1106 and 1025.5 cm^{-1} corresponding to stretching vibration of its C—OH group, 1642 cm^{-1} corresponding to asymmetric stretching vibration of its carboxylate (COO^-) group and 1402 cm^{-1} peak is for symmetrical stretching vibration of its COO^- group (Huaa et al., 2010; Wang & Wang, 2010). The absorption band at 3370 cm^{-1} is due to its hydroxyl (O—H) stretching. The FTIR of CP copolymer gel is shown in Fig. 3B. It shows absorption peaks at 1655 and 3320 cm^{-1} for asymmetric stretching vibration of its carboxylic (COOH) and hydrogen bonded alcohol (O—H). Most of the characteristic absorption peaks of CP gel and sodium alginate is shifted in CPSA4 gel as shown in Fig. 3C. Accordingly, carboxylic asymmetric peak (COOH) of acrylic acid is shifted from 1655 cm^{-1} in CP gel to 1676 cm^{-1} in IPN gel. Absorption band at 1106 and 1025.5 cm^{-1} of alginate corresponding to stretching vibration of its C—OH group shows major shift due to its chemical interaction with the copolymer and the IPN gel shows new absorption peaks at 1136 and 1192 cm^{-1}. However, asymmetric stretching vibration of COO^- group of alginate at 1402 cm^{-1} remains almost same (1400 cm^{-1}) in the IPN. Similarly, SCP gel shows absorption at 3314, 1727 and 1401 cm^{-1} for its hydroxyl (O—H), asymmetric stretching of COO— and symmetrical stretching of COO— (Wang & Wang, 2010) as shown in Fig. 3D. In the SCPSA4 gel C—OH stretching is also shifted to 1136 and 1192 cm^{-1} while asymmetric and symmetric stretching of both alginate and sodium carboxylate is overlapped at 1725 and 1400 cm^{-1}, respectively.

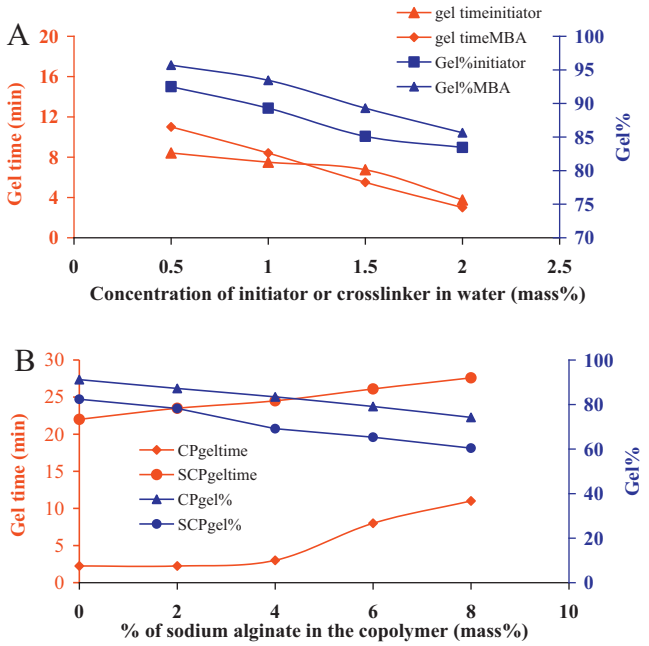

Fig. 2. Variation of gel time and gel% with (A) initiator or crosslinker (MBA) concentration and (B) % of sodium alginate.

3.2.3. Scanning electron microscopy (SEM)

SEM was studied to investigate morphology of the hydrogels. SEM of acrylic acid–hydroxy ethylmethacrylate copolymer (CP, 0% alginate) and its IPN with sodium alginate for 2, 4 and 6% alginate is shown in Fig. 4A–D, respectively. It is evident that the micrographs show increasingly coarser morphology with increase in % of alginate. Surface roughness also increases with generation of pores and gaps in the IPN gels containing 4 and 6% alginates (Fig. 4C and

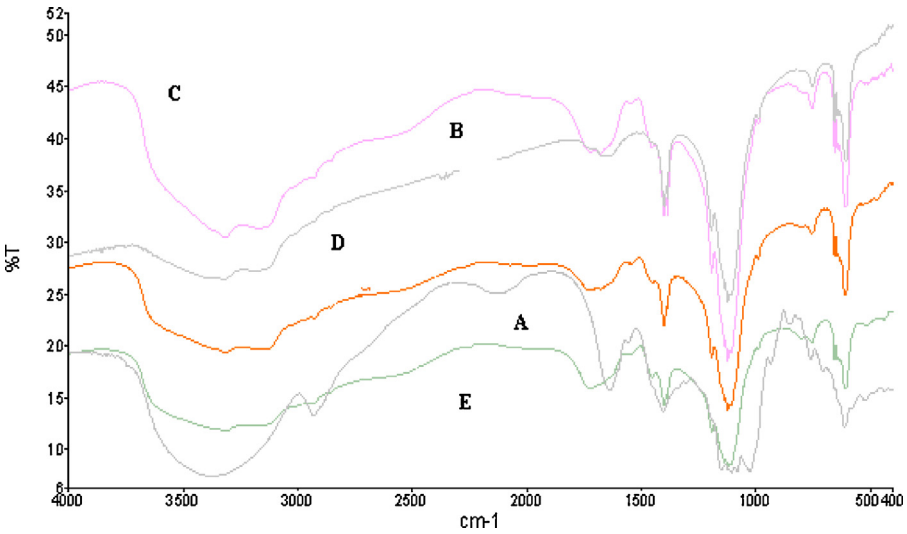

Fig. 3. FTIR of the hydrogels. (A) Sodium alginate, (B) acrylic acid–HEMA copolymer gel, (C) IPN gel of acrylic acid–HEMA copolymer and 4% sodium alginate, (D) sodium acrylate–HEMA copolymer gel, (E) IPN gel of sodium acrylate–HEMA copolymer and 4% sodium alginate.

D). Thus, introduction of alginate facilitates surface and network structure of the IPN gel (Wang & Wang, 2010) which is desirable for good absorption properties.

3.2.4. X-ray diffraction (XRD)

Sodium alginate shows some crystallinity due to hydrogen bonding among its hydroxyl groups. However, during IPN formation with acrylic copolymer, these hydroxyl functional groups of alginate forms chemical bond with copolymers (as it was also evident from free carboxyl % and FTIR analysis) and thus crystalline peaks of diffractogram of sodium alginate is not likely to be present in its IPN with copolymer. XRD of sodium alginate, CP and CPSA4 gel is shown in Fig. 5. From this figure it is observed that sodium alginate shows three crystalline peaks at 14.3°, 21.3° and 37.1° (Dong, Dong, Cao, Han, & Ding, 2011). The copolymer gel (CP), being amorphous shows no crystalline peak. However, the crystalline peaks of alginate are absent in its IPN i.e. in CPSA4, as observed in the same figure.

3.2.5. DTA and TGA

DTA and TGA of CP, CPSA4 and SCPSA4 gel is shown in Fig. 6A and B, respectively. It is observed from the DTA curves that CP shows a glass transition temperature (T_g) of around 78 °C which increases to around 96 °C for SCPSA4. CPSA4 is observed to show the highest T_g of 115 °C. The IPN gels show higher T_g because of interpenetration and crosslinking of two polymers i.e. sodium alginate and the copolymer which resist segmental motion of the polymer chains. The IPN containing sodium salt of copolymer i.e. SCPSA4 shows lower T_g than CP gel which may be due to presence of excess carboxylate anion in its structures. From TGA of the hydrogels as shown in Fig. 6B it is observed that the hydrogels show three weight loss regions with onset of maximum weight loss at its melting temperatures. The weight losses of these hydrogel polymers in different temperature regions are associated with splitting of the main chain and final decomposition of the polymer. It is also observed that the IPN hydrogel shows higher thermal stability than the copolymer gel which may be due to crosslinking and networking of both of the constituent polymer in IPN gels.

3.2.6. Mechanical properties

The TS of the hydrogels increases with increase in % of alginate in the following order CP (33.29 MPa) < CPSA2 (39.33 MPa) < CPSA4 (42.22 MPa) < CPSA6 (47.11 MPa) < CPSA8 (52.11 MPa) while EAB shows an opposite trend i.e. it decreases in the following order CP (53.23%) > CPSA4 (47.11%) > CPSA4 (42.23%) > CPSA6 (38.77%) > CPSA8 (33.78%). The higher TS of the IPN hydrogels may be ascribed to presence of double networks of copolymer and alginate in the IPN. Interpenetration and crosslinking of the polymers increases stiffness and TS of the hydrogel. With increase in % of crystalline sodium alginate, the network becomes increasingly tighter from CPSA2 to CPSA4 with increase in TS. However, stiffness of the hydrogels also decreases its elongation and hence EAB decreases in the opposite order.

3.3. Study of swelling properties of the hydrogels

The variation of water uptake (g of water absorbed/g of gel) of the hydrogels is shown in Fig. 7A–F for varied initiator concentration, crosslinker concentration, sodium alginate % in copolymer, sodium alginate % in sodium salt of copolymer, pH for IPN with copolymer and pH for IPN with sodium salt of copolymer, respectively. From all of these swelling curves it is observed that initially water uptake% increases with time and finally it levels off at an equilibrium value. There is no further increase in water uptake with time above this equilibrium value.

3.3.1. Effect of initiator concentration on swelling

The effect of initiator concentration on swelling of IPN of copolymer and 4% sodium alginate is shown in Fig. 7A. From this swelling curve it is observed that with increasing initiator concentration from 0.5% to 1.5 mass% (of total monomer mass), water uptake% increases for this gel. Similar results were obtained with other hydrogels. Polymerization time was too long below 0.5 mass% of initiator while above1.5 mass% initiator the gel produced was of poor mechanical strength. For all of the hydrogels EWC increases with increasing initiator concentration as shown in Fig. 7A. As initiator concentration increases lower molecular weight gel with more chain ends is formed. This leads to network imperfection in the gel (Chang et al., 2010; Jeon et al., 2008) and hence increased swelling uptake or EWC. In all of the subsequent experiments initiator concentration was fixed at 1 mass%.

3.3.2. Effect of crosslinker concentration on swelling

Effect of concentration of crosslinker i.e. MBA on swelling of IPN hydrogel of copolymer and 4% hydrogel i.e. CPSA4 is shown in Fig. 7B. Similar kind of swelling curves were also obtained with

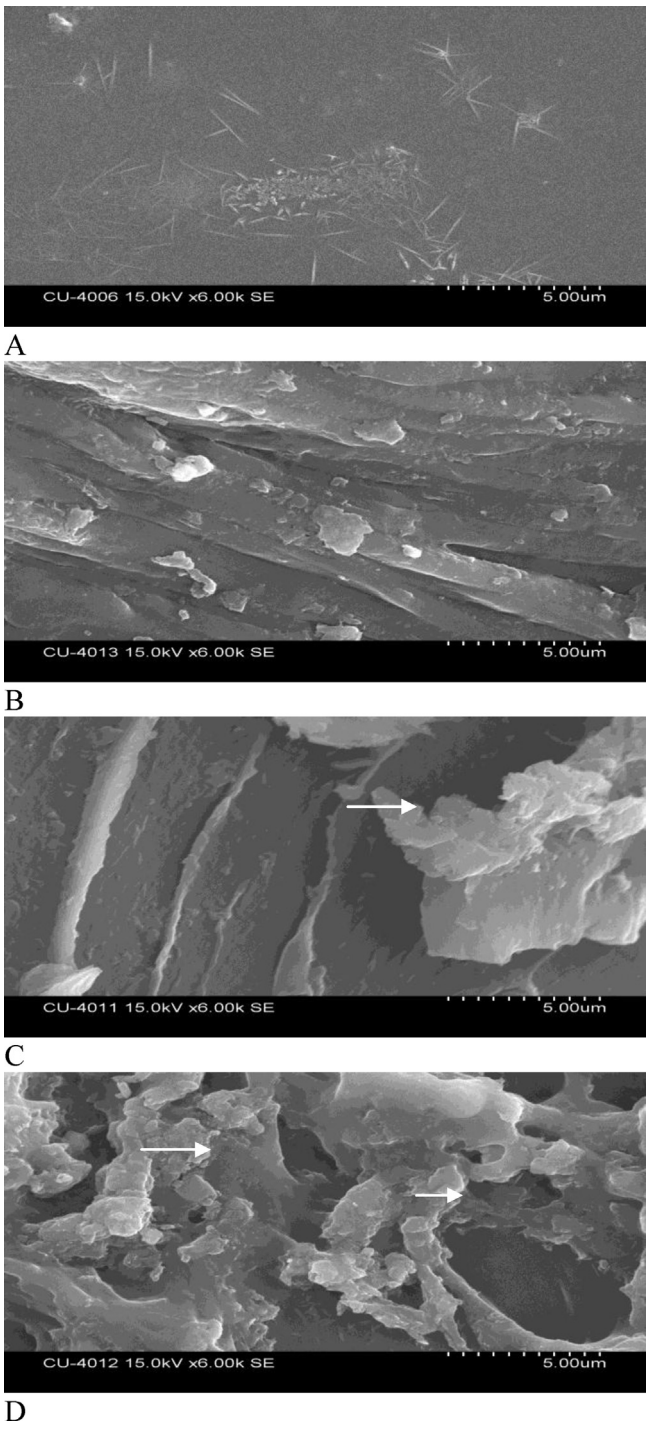

Fig. 4. SEM of the hydrogels (A) copolymer gel, (B) IPN gel with 2% alginate, (C) IPN gel with 4% alginate, (D) IPN gel with 6% alginate (arrow shows rough surfaces).

the other hydrogels. From Fig. 7B it is observed that water uptake or EWC decreases with increase in MBA concentration. In fact, with increase in concentration of crosslinker, network of the gels becomes denser with reduction in water uptake or EWC. However, below 0.5 mass% MBA, no stable network was formed and the resulting polymer was soluble in water. Thus, the initial or the lowest crosslinker concentration was fixed at 0.5 mass% of total monomer.

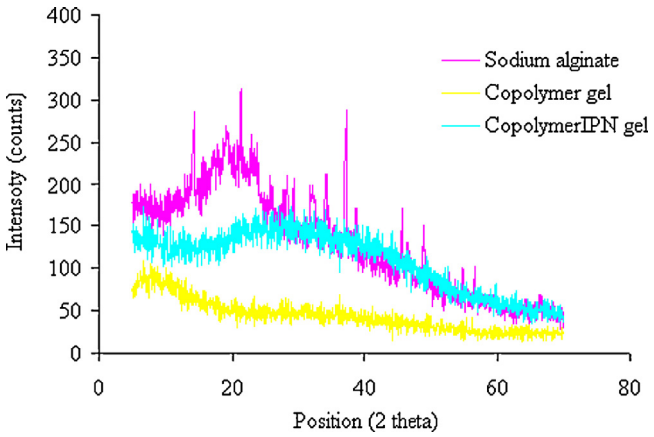

Fig. 5. XRD of hydrogels.

3.3.3. *Effect of sodium alginate % on swelling*

It is observed from Fig. 7C that with increase in mass% of sodium alginate, water uptake as well as EWC of the hydrogels increases up to 4 mass% of alginate and then it decreases. Introduction of hydrophilic polymer like sodium alginate in the gel network of the copolymer increases its water absorption properties. Further, sodium alginate also provides electrostatic repulsive force in the network because of its negatively charged carboxylate functional groups (COO^- Na^+). Thus, water absorption properties of the hydrogel improve with introduction of alginate. However, further increase of alginate (above 4 mass%) decreases swelling properties of the gels which may be due to filling up of the void spaces of the network chains by alginate. Thus, entry of water molecules in the network is reduced (Murali Mohan, Keshava Murthy, & Mohana Raju, 2005). Similar trend of water absorption is also observed with IPN of sodium salt of acrylic acid–hydroxy ethylmethacrylate copolymer containing varied amounts of sodium alginates as observed in Fig. 7D. However, these acrylate copolymer hydrogels shows much higher water absorption than acrylic acid copolymer hydrogels containing same amount of sodium alginate. This may be ascribed to presence of excess negatively charged carboxylate functional groups (COO^- Na^+) which is present in sodium acrylate copolymer as well as in sodium alginate.

3.3.4. *Effect of pH*

As expected, with increase in solution pH swelling ratio and equilibrium water content of the IPN gel of copolymer and alginate increases (Fig. 7E and F) which confirms pH sensitivity of the hydrogels. Hydrogen bonding among the —COOH groups of the copolymer increases at low pH. This results in formation of additional physical networks (Wang & Wang, 2010). On the other hand electrostatic interaction among COO^- groups is also restricted at low pH. Thus, the IPN gels shrink at low pH and show less swelling. At high pH the carboxylic groups are converted to carboxylate anions with expansion of the gel network due to electrostatic repulsion resulting in increased swelling.

3.3.5. *Swelling kinetics and diffusion characteristics*

Equilibrium swelling % (ES %) of the hydrogels was obtained from their corresponding swelling curves. The swelling data were fitted to 2nd order rates (Eq. (4)) to obtain ES% (calculated), initial rate of swelling (r_0) and rate constant (k_{s2}). These kinetic data for various hydrogels are shown in Table 1. The non linear data fitting was carried out by Origin-8 software. The non-linear fitting with this software is based on Levenberg–Marquardt (L–M) algorithm where parameter values of a model are adjusted in an iterative process using chi square (χ^2). The validity of the kinetic model was

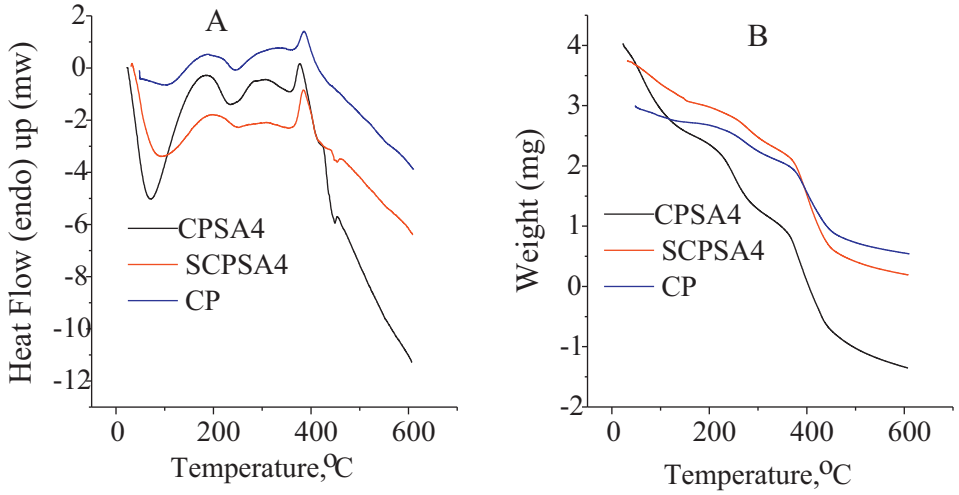

Fig. 6. DTA and TGA of the hydrogels. (A) DTA of the hydrogels and (B) TGA of the hydrogels.

evaluated in terms of regression coefficient (r^2), non linear χ^2 and F values (obtained from Anova analysis in Origin). For a good fitting, r^2 should be close to unity, χ^2 will be low while F value will be high (Yang & Al-Duri, 2005). From Table 1 it is observed that except for Fig. 7E the hydrogels show low χ^2 high 'F' and r^2 close to unity. The values of r^2 and F of Fig. 7E are well within good fitting (Table 1) but its χ^2 values are relatively high which may be due to its variation from multivariate normality (Hooper, Coughlan, & Mullen, 2008). In Table 1 calculated EWC values of the hydrogels are also observed to match closely with experimental EWC. All of these signifies good fitting of swelling data to second order kinetics. From Table 1 it is also observed that with variation of crosslinker, initiator, sodium alginate and copolymer type, there is a significant change of swelling parameters depending on extent of swelling. This may be due to structural change in hydrogels and subsequent variation of polymer–solvent (water) interactions (Murali Mohan et al., 2005). Diffusion characteristics i.e. diffusion constant (k_D), diffusion exponent (n) and diffusion coefficient of the hydrogels as obtained by non linear fitting of swelling data to Eq. (10) and also using Eq. (11) (for obtaining diffusion coefficient) are also shown in Table 1. The values of statistical parameters i.e. r^2, χ^2 and F as also shown in Table 1 indicates good fitting of the swelling data. Here k_D is related to structure of the gel and 'n' is related to kind of transport through the gel. It is observed that hydrogels with varied crosslinker%, initiator% and sodium alginate% shows 'n' values less than or close to 0.5 i.e. these gels show case-I diffusion. This may be ascribed to extensive swelling of these hydrogels for which relaxation due to extensive swelling of the polymers dominates diffusion of water in the network resulting in case-I diffusion. It is also observed that hydrogels containing sodium salt of copolymer and sodium alginate shows values of 'n' greater than 0.5 i.e. case III or non Fickian anomalous diffusion because of comparable swelling and diffusion rate. Diffusion coefficients of the hydrogels are given in Table 1. High diffusion coefficients of water are observed for the IPN type gels.

3.4. Network parameters

Average molecular weight between crosslinks ($\bar{M}$), crosslink density (ρ_c) and mesh size (ς) of the various hydrogels are also shown in Table 1. It is observed that with increase in crosslinker concentration, $\bar{M}$ and ς decreases while ρ_c increases. This may be attributed to the formation of increased number of networks in the structure of gel with increase in crosslinker concentration. With increase in initiator concentration molecular weight of the polymer decreases (Odian, 1991) and hence both $\bar{M}$ and ς decreases while ρ_c increases. It is also observed that with increase in % of sodium alginate in the IPN of copolymer and also sodium salt of copolymer, $\bar{M}$ and ς of the hydrogel increases. This may be due to the formation of more branched multiple side chains in the hydrogels (Wang & Wang, 2010). However, above 6 mass% alginate, $\bar{M}$ and ς decreases which may be due to increase in viscosity of polymerization solution for which initiation efficiency of alginate greatly decreases. Consequently influence of alginate on network parameters also reduces (Wang & Wang, 2010).

3.5. Effect of feed concentration on dye removal% and dye adsorption

Dye removal% of the four hydrogels i.e. copolymer of acrylic acid and hydroxy ethylmethacrylate (CP), copolymer of sodium acrylate and hydroxy ethylmethacrylate (SCP) and IPN of these two copolymers with 4% alginate (CPSA4 and CPSSA4, respectively) for both Congo red and methyl violet dyes are shown in Fig. 8A and B, respectively. Dye adsorption experiments were done at pH 7 since above this pH the increase in dye adsorption was marginal. Among all of the IPN hydrogels only CPSA4 and CPSSA4 were chosen since these hydrogels showed the highest EWC. It is observed from Fig. 8A and B that the hydrogels show very high adsorption for these two industrially important dyes. Thus, over the feed dye concentration range of 10–140 mg/L, the copolymer gel (CP) is observed to show 38–80% adsorption of Congo red which is increased to 45–85% for SCP, 49–94% for CPSA4 and 55–97.6% for CPSSA4 gel. In a similar way the CP, SCP, CPSA4 and CPSSA4 gel shows 36–67%, 38–80%, 40–90% and 47–95% removal of methyl violet dye, respectively for same range of feed dye concentration. The higher adsorption or removal% for Congo red may be due to structural difference (Fig. 1) of these two dye. Congo red contains two primary amine functional groups which protonates at experimental pH (7) and thus show strong electrostatic interactions with various functional groups of hydrogels. On the other hand methyl violet contains tertiary amine group. Thus, Congo red–hydrogel electrostatic interaction will be higher than methyl violet–hydrogel interaction (Bayramoglu, Altintas, & Yakup Arica, 2009) resulting in higher adsorption for Congo red. It is also observed from Fig. 8A and B that initially dye removal% increases with feed concentration, reaches a maximum and then decreases. A given amount of hydrogel can adsorb a fixed amount of dye molecules. As the feed concentration increases, the % of this fixed amount decreases with respect to increased feed concentration and hence dye removal%

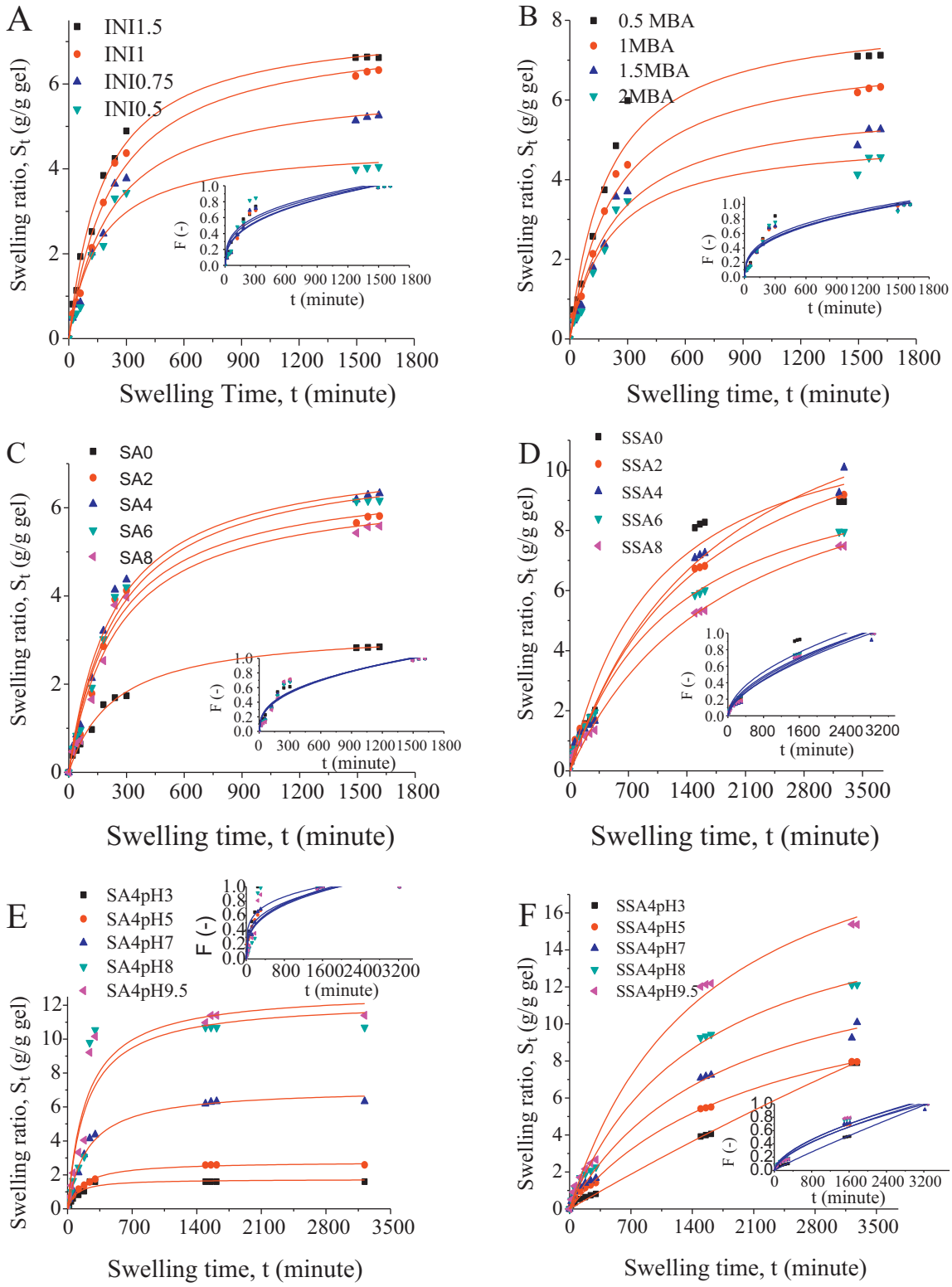

Fig. 7. Direct fitting of swelling data to 2nd order rate equation ($S_t = W_e^2 k_{S2} t/(1 + k_{S2} W_e t)$) for varied (A) initiator concentration, (B) crosslinker concentration, (C) sodium alginate % in copolymer, (D) sodium alginate % in sodium salt of copolymer, (E) pH for IPN with copolymer and (F) pH for IPN with sodium salt of copolymer. Direct fitting to diffusion kinetics curves ($F = kt^n$) are shown in insets.

decreases at higher feed dye concentration. The variation of dye adsorption (Q_e, mg dye/g gel) with feed concentration (C_e) is shown in Fig. 8C for Congo red and 8D for methyl violet dye. It is observed that dye adsorption increases with feed concentration and above a certain concentration (~100 mg/L) the change in dye adsorption is marginal. The increase in dye adsorption with feed concentration may be ascribed to decrease in mass transfer resistance of dye molecules (Bayramoglu et al., 2009; Bhattacharyya, Ray, & Mandal, 2012) between solid (hydrogel) and liquid (dye solution). However, as the hydrogel molecules are saturated with dye

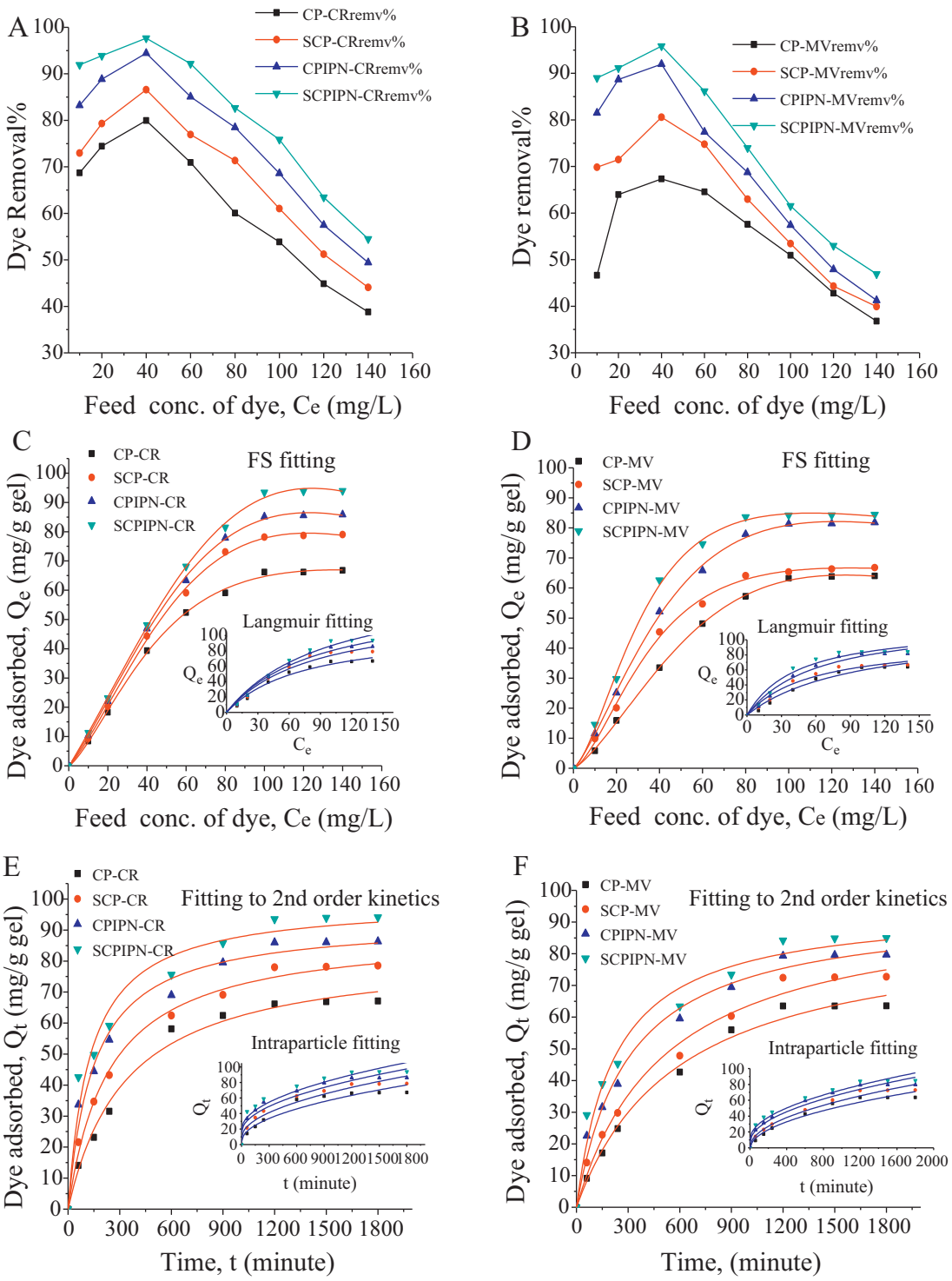

Fig. 8. (A) Dye removal% of hydrogels for Congo red (CR) and (B) for methyl violet (MV) dye, (C) direct non linear data fitting to four-parameter Fritz–Schlünder (FS) and two-parameter Langmuir (inset)adsorption isotherm model for CR and (D) MV dye. (E) Direct non linear data fitting to 2nd order and intra particle (inset) kinetics for CR and (F) for MV dye.

molecules, there is no further increase in adsorption at higher feed concentration.

3.5.1. *Fitting of dye adsorption data to adsorption isotherms and kinetics*

In Fig. 8B and C dye adsorption data were also fitted to two-parameter Langmuir (Eq. (13)) and four-parameter Fritz–Schlünder (FS) (Eq. (14)) model. In Fig. 8D and E dye adsorption at various time intervals were fitted to pseudo 2nd order kinetics (Eq. (15)) and intra particle diffusion (Eq. (16)). Various model parameters along with statistical parameters of error analysis for these non linear fittings are shown in Table 2. It is evident from these models and statistical parameter values that the dye adsorption closely fits Langmuir or Fritz–Schlünder isotherm and also second order and intra particle kinetics though χ^2 values of some of these fittings are observed to be relatively high which may be due to

Table 2
Kinetic parameters of the Hydrogels for CR and MV dye.

Model	CP-CR/MV	SCP-CR/MV	CPIPN-CR/MV	SCPIPN-CR/MV
Pseudo 2nd				
Q_{eth} (mg/g)	83.21/88.52	89.83/96.72	93/94.4	83.21/88.52
k_2 (g/mg min)	3.57E−05/1.92E−05	4.64E−05/2E−05	7.14E−05/3.5E−05	3.6E−05/1.9E−05
r^2	0.9883/0.9913	0.9942/0.9877	0.9831/0.9855	0.9883/0.9913
χ^2	8.02/5.62	4.67/9.5	14.9/12.26	32.4/22.8
F value	1389/1601	3263/1224	1319/1234	726/771
Intraparticle				
k_p (mg/g min$^{1/2}$)	1.72/1.7	1.88/1.87	1.93/1.94	2.04/1.97
c	3.95/1.05	8.81/0.921	15.89/6.82	19.39/10.94
r^2	0.92971/0.9673	0.9436/0.9782	0.9043/0.9628	0.8914/0.9503
χ^2	48.3/21.2	45.5/16.9	84.6/31.6	109/44
F value	227/422	331/686	229/477	213/397
Langmuir				
K_L (l/mg)	0.014/0.011	0.012/0.018	0.012/0.016	0.01/0.02
Q_{max} (mg/g)	108.95/115.48	135/100	149.68/126.18	172/120
R_L	0.0071/0.0072	0.0070/0.0072	0.0072/0.0071	0.0072/0.0071
r^2	0.9800/0.9756	0.9765/0.9710	0.9792/0.9758	0.9817/0.9651
χ^2	14.09/16.55	23.91/20.53	24.8/25.8	25.91/39.5
F value	756/575	620/551	698/651	780/488
FS				
A_{FS}	863/5075	11730/342	34398/1730	219679/490
α	−0.46/−0.80	−0.92/−0.299	−1.102/−0.56	−1.43/−0.33
B_{FS}	2065/14844	19115/1096	43500/2622	223666/1003
β	−1.76/−2.08	−2.10/−1.77	−2.22/−1.81	−2.49/−1.78
r^2	0.9985/0.9995	0.9988/0.9968	0.9991/0.9987	0.9989/0.9978
χ^2	1.03/0.34	1.27/2.28	1.027/1.385	1.44/2.45
F value	5185/14073	5854/2500	8472/6103	7059/3971

deviation of some experiments from normality (Hooper et al., 2008).

3.6. Thermodynamics of dye adsorption

The change in free energy (ΔG) during dye adsorption is obtained as

$$\Delta G = \Delta G^0 + RT \ \ln K_d \tag{17}$$

where ΔG^0 is change in standard free energy and K_d is distribution coefficient of dye between hydrogel and solution which is obtained from equilibrium dye adsorption (Q_e) and feed dye concentration (C_e) value as

$$K_d = \frac{Q_e}{C_e} \tag{18}$$

$$\text{At equilibrium,} \quad \Delta G = 0, \quad \text{Hence,} \quad \Delta G^0 = -RT \ln K_d \tag{19}$$

Further, distribution coefficient of dye adsorption at different temperatures is related to standard enthalpy (ΔH^0) or entropy change (ΔS^0) as (Bhattacharyya et al., 2012).(20)$\ln K_d = -\frac{\Delta H^0}{RT} + \frac{\Delta S^0}{R} K_d$ at three different temperatures i.e. 25, 35 and 50 °C were obtained from dye adsorption data at these three temperatures for 100 mg/L feed concentration of Congo red and methyl violet dye using Eq. (18). ΔH^0 and ΔS^0 were obtained from slope and intercept, respectively of linear plot of $\ln K_d$ against inverse of absolute temperature ($1/T$). ΔG^0 values were found to be negative (−15.2/−15, −15.6/15.1, −15.8/15.7 and −16/15.8 kJ for CP, SCP, CPSA4 and SCPSA4 hydrogel, respectively, for 100 mg/L Congo red/methyl violet dye at 25 °C) which confirms feasibility, spontaneity and physisorption of this dye adsorption process (Wang, Zeng, Ren, Song, & Wang, 2010). Positive values (3/3.4, 2.72/3.6, 2.91/3.4 and 1.79/3.3 kJ for CP, SCP, CPSA4 and SCPSA4 hydrogel, respectively, for 100 mg/L Congo red/methyl violet) of ΔH^0 confirms the exothermic nature of the adsorption. ΔS^0 was also found to be positive (0.06/0.061, 0.061/0.063, 0.063/0.064 and 0.059/0.064 kJ for CP, SCP, CPSA4 and SCPSA4 hydrogel, respectively, for 100 mg/L Congo red/methyl violet) which indicates increase in randomness in the solid (gel)–dye solution interface during adsorption. These values of thermodynamic parameters are also comparable to those reported elsewhere (Bhattacharyya et al., 2012; Wang et al., 2010; Kayranli, 2011).

3.7. Reusability of hydrogels

Desorption of dye loaded hydrogels at pH 7 was not significant while the hydrogels showed very high desorption (up to 97%) at pH 3.5 indicating strong electrostatic interaction between dye and hydrogel (Banat et al., 1996). The regenerated hydrogels was used for five repeated adsorption/desorption cycles without any significant change of adsorption% indicating reusability of the hydrogels.

4. Conclusion

Several hydrogels were synthesized from copolymer of acrylic acid, sodium acrylate, hydroxyethyl methacrylate and sodium alginate. These copolymer and IPN type hydrogels were crosslinked with MBA. All of the hydrogels were characterized with free carboxylic %, FTIR, SEM, XRD, DTA–TGA and mechanical properties. Swelling, diffusion and network parameters of the hydrogels were evaluated. Among all the hydrogels CP, SCP, CPSA4 and SCP4 showing high swelling in water were used for removal of Congo red and methyl violet dye from water. All of these four hydrogels showed high adsorption and removal% of these two dyes. Experimental dye adsorption data were found to closely fit two adsorption isotherms i.e. two-parameter Langmuir and four-parameter Fritz–Schlünder model and also pseudo second order kinetics and intra particle diffusion. Various thermodynamic parameters indicated spontaneity, feasibility and exothermic nature of the dye adsorption. These hydrogels may also be used for removal of other similar dyes from water.

Acknowledgement

The authors are grateful to Council of Scientific and Industrial Research (CSIR), Govt. of India for sponsoring this work.

References

Banat, I., Nigam, P., Singh, D., & Marchant, R. (1996). Microbial decolorization of textile dye-containing effluents: A review. *Bioresource Technology*, *58*, 217–227.

Bayramoglu, G., Altintas, B., & Yakup Arica, M. (2009). Adsorption kinetics and thermodynamic parameters of cationic dyes from aqueous solutions by using a new strong cation-exchange resin. *Chemical Engineering Journal*, *152*, 339–346.

Bhattacharyya, R., Ray, S. K., & Mandal, B. (2012). A systematic method of synthesizing composite superabsorbent hydrogels from crosslink copolymer for removal of textile dyes from water. *Journal of Industrial and Engineering Chemistry*, *19*(2013), 1191–1203.

Canal, T., & Peppas, N. A. (1989). Correlation between mesh size and equilibrium degree of swelling of polymeric networks. *Journal of Biomedical Materials Research*, *23*(10), 1183–1193.

Chang, C., Duan, B., Cai, J., & Zhang, L. (2010). Superabsorbent hydrogels based on cellulose for smart swelling and controllable delivery. *European Polymer Journal*, *46*, 92–100.

Chen, J., Park, H., & Park, K. (1999). Synthesis of super porous hydrogels: Hydrogels with fast swelling and superabsorbent properties. *Journal of Biomedical Materials Research*, *44*, 53–62.

Dilek, S., Murat, T., & Guven, O. (2008). The usability of (sodium alginate/acrylamide) semi-interpenetrating polymer networks on removal of some textile dyes. *Journal of Applied Polymer Science*, *108*, 3787–3795.

Dong, Y., Dong, W., Cao, Y., Han, Z., & Ding, Z. (2011). Preparation and catalytic activity of Fe alginate gel beads for oxidative degradation of azo dyes under visible light irradiation. *Catalysis Today*, *175*, 346–355.

Fritz, W., & Schlunder, E. (1974). Simultaneous adsorption equilibria of organic solutes in dilute aqueous solution on activated carbon. *Chemical Engineering Science*, *29*, 1279–1282.

Hooper, D., Coughlan, J., & Mullen, M. R. (2008). Structural equation modelling: Guidelines for determining model fit. *Electronic Journal of Business Research Methods*, *6*, 53–60. Available at: www.ejbrm.com

Ho, Y., & McKay, G. (1999). Pseudo second-order model for sorption processes. *Process Biochemistry*, *34*, 451–465.

Horia, M., Nizam, E. D., Manal, F., Abou, T., Wahab, A., & El-Naggar, M. (2008). Metal sorption and swelling characters of acrylic acid and sodium alginate based hydrogels synthesized by gamma irradiation. *Nuclear Instruments and Methods in Physics Research B*, *266*, 2607–2613.

Huaa, S., Mac, H., Xun, L. C., Yanga, H. B., & Wanga, A. (2010). pH-sensitive sodium alginate/poly(vinyl alcohol) hydrogel beads prepared by combined Ca^{2+} crosslinking and freeze-thawing cycles for controlled release of diclofenac sodium. *International Journal of Biological Macromolecules*, *46*, 517–523.

Jeon, Y. S., Lei, J., & Kim, J. H. (2008). Dye adsorption characteristics of alginate/polyaspartate hydrogels. *Journal of Industrial and Engineering Chemistry*, *14*, 726–731.

Kayranli, B. (2011). Adsorption of textile dyes onto iron based waterworks sludge from aqueous solution: Isotherm, kinetic and thermodynamic study. *Chemical Engineering Journal*, *173*, 782–791.

Kulkarni, R. V., Sreedhara, V., Mutalikb, S., Setty, C. M., & Sa, B. (2010). Interpenetrating network hydrogel membranes of sodium alginate and poly(vinyl alcohol) for controlled release of prazosin hydrochloride through skin. *International Journal of Biological Macromolecules*, *47*, 520–527.

Langmuir, L. (1918). The adsorption of gases on plane surfaces of glass, mica, and platinum. *Journal of American Chemical Society*, *40*, 1361–1403.

Li, X., Xu, S., Wang, J., Chen, X., & Feng, S. (2009). Structure and characterization of amphoteric semi-IPN hydrogel based on cationic starch. *Carbohydrate Polymers*, *75*, 688–693.

Mall, I. D., Srivastava, V. C., Kumar, G. V. A., & Mishra, I. M. (2006). Characterization and utilization of mesoporous fertilizer plant waste carbon for adsorptive removal of dyes from aqueous solution. *Colloids and Surfaces A: Physicochemical and Engineering Aspects*, *278*, 175–187.

Mandal, B., Ray, S. K., & Bhattacharyya, R. (2012). Synthesis of full and semi interpenetrating hydrogel from polyvinyl alcohol and poly (acrylic acid-co-hydroxyethylmethacrylate) copolymer: Study of swelling behavior, network parameters, and dye uptake properties. *Journal of Applied Polymer Science*, *124*, 2250–2268.

Morris, E. R., Cutler, A. N., Ross-Murphy, S. B., Rees, D. A., & Price, J. (1981). Concentration and shear rate dependence of viscosity in random coil polysaccharide solutions. *Carbohydrate Polymers*, *1*, 5–21.

Murali Mohan, Y., Keshava Murthy, P. S., & Mohana Raju, K. (2005). Synthesis, characterization and effect of reaction parameters on swelling properties of acrylamide–sodium methacrylate superabsorbent copolymers. *Reactive & Functional Polymers*, *63*, 11–26.

Murthy, P. S. K., Murali Mohan, Y., Sreeramulu, J., & Mohana Raju, K. (2006). Semi-IPNs of starch and poly(acrylamide-co-sodium methacrylate): Preparation, swelling and diffusion characteristics evaluation. *Reactive & Functional Polymers*, *66*, 1482–1493.

Odian, G. (1991). Radical chain polymerization. In *Principle of polymerization* (third ed., pp. 198–334). Singapore: John Wiley & Sons Inc.

Paul, J. F., & John, R. J. (1943). Statistical mechanics of cross-linked polymer networks: I. Rubber like elasticity. *Journal of Chemical Physics*, *11*, 512–517.

Peppas, N. A., Hilt, J. Z., Ali, K., & Robert, L. (2006). Hydrogels in biology and medicine: From molecular principles to bionanotechnology. *Advanced Materials*, *18*, 1345–1360.

Ritger, P. L., & Peppas, N. A. (1987). A simple equation for description of solute release I Fickian and non-Fickian release from non-swellable devices in the form of slabs, spheres, cylinders or discs. *Journal of Controlled Release*, *5*, 23–36.

Sunil, K. B., & Surinderpal, S. (2006). Analysis of swelling behaviour of poly (methacrylamide-co-methacrylic acid) hydrogels and effect of synthesis conditions on water uptake. *Reactive & Functional Polymers*, *66*, 431–440.

Tang, Q., Sun, X., Li, Q., Wu, J., & Lin, J. (2009). A simple route to interpenetrating network hydrogel with high mechanical strength. *Journal of Colloid and Interface Science*, *339*, 45–52.

Wang, Y., Zeng, L., Ren, X., Song, H., & Wang, A. (2010). Removal of methyl violet from aqueous solutions using poly(acrylic acid-co-acrylamide)/attapulgite composite. *Journal of Environmental Sciences*, *22*(1), 7–14.

Wang, L., Zhang, J., & Wang, A. (2011). Fast removal of methylene blue from aqueous solution by adsorption onto chitosan-g-poly (acrylic acid)/attapulgite composite. *Desalination*, *266*, 33–39.

Wang, W., & Wang, A. (2010). Synthesis and swelling properties of pH-sensitive semi-IPN superabsorbent hydrogels based on sodium alginate-g-poly(sodium acrylate) and polyvinylpyrrolidone. *Carbohydrate Polymers*, *80*, 1028–1036.

Weber, W., & Morris, J. (1963). Kinetics of adsorption on carbon from solution. *Journal Sanitary Engineering Division. American Society Civil Engineering*, *89*, 31–59.

Xue, W., Champ, S., & Huglin, M. B. (2001). Network and swelling parameters of chemically crosslinked thermoreversible hydrogels. *Polymer*, *42*, 3665.

Yang, X., & Al-Duri, B. (2005). Kinetic modeling of liquid-phase adsorption of reactive dyes on activated carbon. *Journal of Colloid and Interface Science*, *287*, 25–34.

Yin, Y., Ji, X., Dong, H., Ying, Y., & Zheng, H. (2008). Study of the swelling dynamics with overshooting effect of hydrogels based on sodium alginate-g-acrylic acid. *Carbohydrate Polymers*, *71*, 682–689.